JOURNAL OF GUIDANCE, CONTROL, AND DYNAMICS
Vol. 25, No. 3, May–June 2002

Time-Varying Linear Pursuit–Evasion Game Models with Bounded Controls

Tal Shima* and Josef Shinar†
Technion—Israel Institute of Technology, 32000 Haifa, Israel

Future end game interception scenarios of autonomous uncrewed flying vehicles are expected to be characterized by variable velocities and lateral acceleration limits. A time-varying linear pursuit–evasion game model with bounded controls is presented that can be used to analyze such scenarios. The usefulness of this model is demonstrated by simulations of a realistic ballistic missile defense scenario, as an example. It is shown that a differential game guidance law derived using this time-varying model provides a significant improvement in the homing accuracy compared to a guidance law based on a model with constant velocities and lateral acceleration limits. Moreover, the time-varying linear model provides a much more accurate prediction of the miss distance, confirming its validity. Also a general review of possible structures of the game space decomposition is presented. One of these structures implies that even if the pursuer does not have a maneuverability advantage over the evader, but has an agility advantage, a zero miss distance can still be achieved for some initial conditions.

Introduction

IN spite of the well-known fact that missile/target interception scenarios are generally characterized by nonlinear kinematics and time-varying velocities, most missile guidance laws have been developed using linearized two-dimensional models assuming constant speeds and lateral acceleration limits. Nevertheless, it turned out that the implementation of these guidance laws in a realistic environment can be successful. The discrepancy between the simplified model and the complex reality has been expressed, however, by the suboptimality of the guidance solution and an inaccurate prediction of the interception outcome.

In a recent paper,[1] the results derived from linearized guidance theory were compared to the outcome of three-dimensional point mass simulations dealing with an interception scenario against a highly maneuvering tactical ballistic missile (TBM). This comparison clearly showed that currently used linear guidance theory does not predict well the miss distance in such real world engagements. The discrepancies between the results have been attributed to the time-varying velocities and lateral acceleration limits of both missiles. Although the assumptions of constant velocities and lateral acceleration limits were found to be invalid, the linearization of the trajectories with respect to the initial line of sight seemed to be well justified. The linearization turned out to be valid due to the very high velocities of both missiles that enabled only a small rotation of the line of sight (LOS) throughout the short duration of the end game.

In the open technical literature there are several works addressing the guidance problem of variable speed missiles. In the book by Garnell,[2] the well-known proportional navigation (PN) guidance law[3] is modified due to the longitudinal acceleration. The correction term is included into the LOS rate needed for the implementation of PN. However, this correction term is by no means optimal, and it also does not null the LOS rate for a variable speed missile. Baba et al.[4] used a different approach. They assumed that the velocity profile of the interceptor is known and guided the missile on a collision course to the future interception point. The performance of this guidance law was evaluated, and it was found that such an interception requires much smaller lateral acceleration of the interceptor than PN.

Optimal control theory assuming unbounded controls has also been used for the derivation of guidance laws for this problem. Riggs[5] used an optimal guidance law derived for the constant speed scenario and estimated the time to go based on the range, varying velocity and the angle between the velocity vectors and the initial LOS. Lee[6] used a similar approach, but computed the time to go optimally. A simulation study of a scenario with a nonmaneuvering target showed the superiority of this guidance law to the conventional PN and to Riggs guidance law.[5] Cho et al.[7] considered the variable velocity of the pursuer from the outset of the optimal control derivation. They found a new guidance law that had the same structure as the augmented PN[8] derived for the constant speed model. It used a time-varying guidance gain, and the computation of the time to go was based also on the knowledge of the future missile velocity profile.

Formulating the interception of a maneuverable target as an optimal control problem, as done in the cited papers, requires an assumption of the future evolution of the maneuver. If the assumption about the target maneuver is correct and the lateral acceleration of the interceptor does not saturate, such a guidance law can reduce the miss distance to zero. However, if the assumption about the target behavior is wrong, very large miss distances are created. Because the target maneuvers are independently controlled, the scenario has to be formulated as a zero-sum pursuit–evasion game. Such a formulation of a scenario between two players with constant velocities and constant bounds on the lateral accelerations assuming ideal dynamics for both players has been investigated by Gutman and Leitmann.[9] This scenario was later extended to include first-order pursuer dynamics[10] and evader dynamics.[11] Gazit and Gutman[12] developed a guidance law for a pursuer with a constant acceleration, using a time-varying linear model assuming for both players ideal dynamics and constant bounded controls. For the case of a nonmaneuvering evader, an optimal control derivation was used, whereas for a maneuvering evader, a differential game approach was employed. The obtained guidance law steers the missile toward a straight-line collision course and enables interception in scenarios where the classical PN fails.

None of these works have addressed the problem of our interest, namely, the scenario where both the interceptor and the target have variable velocities and lateral acceleration limits. The objective of this paper is to extend the frequently used linear game model with bounded controls and first-order dynamics[11] to include known

Received 19 September 2000; revision received 19 June 2001; accepted for publication 6 September 2001.

*Doctoral Student, Faculty of Aerospace Engineering; currently, System Engineer, RAFAEL, P.O.Box 2250, Department 35, 31021 Haifa, Israel. Member AIAA.

†Professor, Max and Lottie Dresher Chair of Aerospace Performance and Propulsion, Faculty of Aerospace Engineering; aer4301@aerodyne.technion.ac.il. Fellow AIAA.

time-varying velocities and lateral acceleration bounds for both players. As an example of this model, a planar TBM interception scenario is used.

In the next section, the new linear time-varying model of an interception scenario is formulated as a perfect information zero-sum pursuit–evasion game. The general solution of this model is presented in the sequel. It is followed by the description of a simplified example illustrating a typical ballistic missile defense (BMD) scenario with time-varying interceptor velocity and TBM lateral acceleration limit. The guidance law based on the model of this simplified example is tested in a three-dimensional nonlinear point-mass simulation using generic, but realistic, data. The solution of the linear game model with constant maneuverability and velocity[11] is reviewed in the Appendix for the sake of completeness.

Problem Formulation

This paper deals with time-varying linear pursuit–evasion game models for realistic interception scenarios, such as an endoatmospheric interception of a maneuverable TBM. During the end game of this interception scenario, the altitude and the velocity of the reentering TBM, as well as of the interceptor missile, are continuously varying. Therefore, their lateral acceleration limits are also changing. In this section a linear time-varying mathematical model of such an interception end game is formulated. This planar model is based on the following set of assumptions:

1) Both missiles can be represented by point masses with linear control dynamics.

2) The relative end game trajectory can be linearized around a fixed reference line, such as the initial LOS.

3) The velocity profiles of both missiles on a nominal trajectory are known and can be expressed as the function of time.

4) The lateral acceleration limit of each missile is known as a function of time.

5) The maneuvering dynamics of the interceptor and the TBM can be approximated by first-order transfer functions with time constants τ_P and τ_E, respectively.

6) The information structure is perfect.

The assumption of perfect information, assumption 6, includes two parts: 1) the designers of both missiles have perfect knowledge of the engagement parameters and 2) both missiles can accurately measure all of the state variables. The second part represents the worst case for the interceptor. In reality, the TBM has no information on the interceptor's state variables, but it can maneuver randomly having a nonzero probability to carry out a very close realization of the optimal deterministic interception avoidance strategy.

Typical velocity profiles for both missiles, obtained in a previous study,[1] are shown in Fig. 1. It can be seen that during the end game the speed of the TBM remains almost unchanged. As a consequence, its maneuverability (used as a synonym for the lateral acceleration limit) is monotonically increasing due to the larger air density in the lower altitudes. The velocity of the interceptor is monotonically

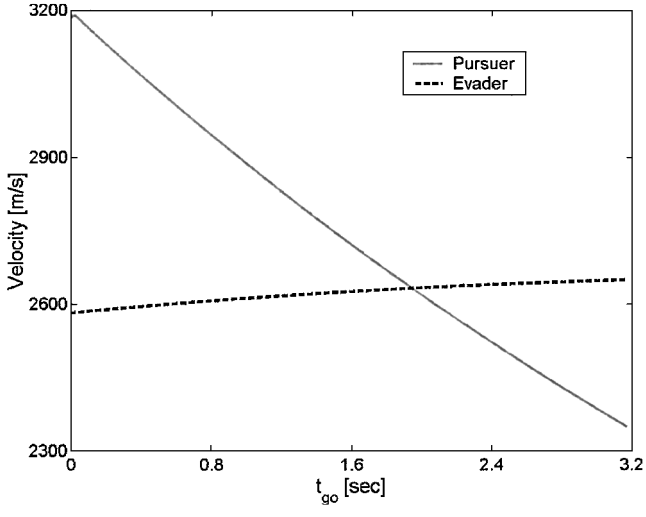

Fig. 1 End-game velocity profiles.

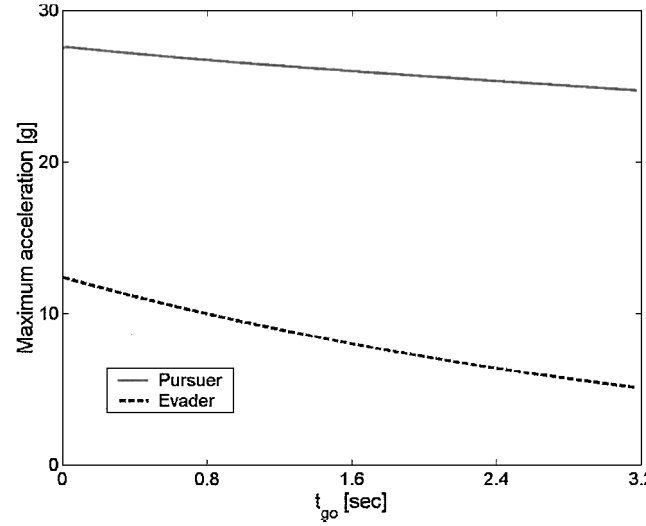

Fig. 2 Time histories of end-game maneuverability.

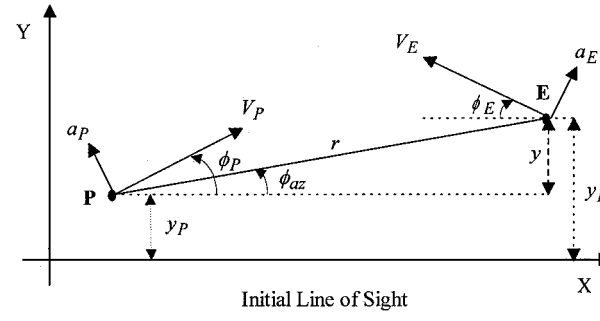

Fig. 3 Planar end-game geometry.

increasing in the end game, because its design has been aimed to keep the end-game maneuverability almost constant, in spite of the increasing altitude and the resulting lower air density. The maneuverability profiles of both missiles are shown in Fig. 2 and can be expressed as the function of time (or time to go).

In Fig. 3, a schematic view of the two-dimensional end-game geometry is shown. Note that the respective velocity vectors of the missiles are generally not aligned with the reference line, which is the initial LOS. The angles ϕ_p and ϕ_E are, however, small. Thus, the approximations $\cos(\phi_i) \approx 1$, $\sin(\phi_i) \approx \phi_i$, $i = P, E$, are uniformly valid and coherent with assumption 2. Nevertheless, the longitudinal accelerations of each missile have nonnegligible components normal to the LOS.

Based on assumptions 2 and 3, the final time of the interception can be computed for any given initial conditions of the end game,

$$t_f = \arg\left\{ X_f = X_0 - \int_{t_0}^{t_f} [V_e(t) + V_p(t)]\,\mathrm{d}t = 0 \right\} \tag{1}$$

allowing the time to go to be defined by

$$t_{\mathrm{go}} \triangleq t_f - t \tag{2}$$

The state vector in the equations of the linearized relative motion normal to the initial LOS is

$$\boldsymbol{X} = [x_1, x_2, x_3, x_4, x_5, x_6]^T = [y, \dot{y}, a_P, a_E, \phi_P, \phi_E]^T \tag{3}$$

where

$$y = y_e - y_p \tag{4}$$

$$\dot{y} = V_E(t)x_6 - V_p(t)x_5, \qquad y(t_0) = y_0 = 0 \tag{5}$$

From the known velocity profiles $V_P(t)$ and $V_E(t)$ the respective longitudinal accelerations $a_{xP}(t)$ and $a_{xE}(t)$ can be computed and substituted into the equations of motion, which become

$$\dot{\boldsymbol{X}} = \boldsymbol{A}(t)\boldsymbol{X} + \boldsymbol{B}(t)u + \boldsymbol{C}(t)v, \qquad \boldsymbol{X}(0) = \boldsymbol{X}_0 \tag{6}$$

with

$$\boldsymbol{A}(t) = \begin{bmatrix} 0 & 1 & 0 & 0 & 0 & 0 \\ 0 & 0 & -1 & 1 & -a_{xP}(t) & a_{xE}(t) \\ 0 & 0 & -1/\tau_P & 0 & 0 & 0 \\ 0 & 0 & 0 & -1/\tau_E & 0 & 0 \\ 0 & 0 & 1/V_p(t) & 0 & 0 & 0 \\ 0 & 0 & 0 & 1/V_E(t) & 0 & 0 \end{bmatrix} \tag{7}$$

$$\boldsymbol{B}(t) = \begin{bmatrix} 0 & 0 & a_P^{\max}(t)/\tau_P & 0 & 0 & 0 \end{bmatrix}^T \tag{8}$$

$$\boldsymbol{C}(t) = \begin{bmatrix} 0 & 0 & 0 & a_E^{\max}(t)/\tau_E & 0 & 0 \end{bmatrix}^T \tag{9}$$

and the normalized controls

$$u = a_p^c / a_p^{\max}(t), \qquad |u| \le 1 \tag{10}$$

$$v = a_E^c / a_E^{\max}(t), \qquad |v| \le 1 \tag{11}$$

where $\boldsymbol{a}_P^c$ and $\boldsymbol{a}_E^c$ are the commanded lateral accelerations for each missile having maximum values that can be expressed as a function of time as $a_P^{\max}(t)$ and $a_E^{\max}(t)$, respectively.

The natural cost function of this perfect information game is the miss distance,

$$J = \left|\boldsymbol{D}^T X(t_f)\right| = |x_1(t_f)| \tag{12}$$

where

$$\boldsymbol{D} = (1, 0, 0, 0, 0, 0)^T \tag{13}$$

By the use of $\Phi(t_f, t)$, the well-known transition matrix of the original homogeneous system $[\dot{\boldsymbol{X}} = \boldsymbol{A}(t)\boldsymbol{X}]$, the transformation of terminal projection is introduced

$$Z(t) = \boldsymbol{D}^T \Phi(t_f, t) X(t) \tag{14}$$

The new scalar state variable Z has the physical interpretation of the zero effort miss distance, and its explicit form is given in the sequel. This transformation allows reducing the vector equation (6) to a scalar dynamic equation in the form

$$\dot{Z} = B(t_f, t)u + C(t_f, t)v \tag{15}$$

where

$$B(t_f, t) = \boldsymbol{D}^T \Phi(t_f, t)\boldsymbol{B}(t) \tag{16}$$

$$C(t_f, t) = \boldsymbol{D}^T \Phi(t_f, t)\boldsymbol{C}(t) \tag{17}$$

whereas the cost function given in Eq. (12) becomes

$$J = |Z(t_f)| \tag{18}$$

General Game Solution

Necessary Conditions of Optimality

The perfect information linear differential game with bounded controls, formulated by Eqs. (15–18), is solved in this section in the most general form.

The Hamiltonian of the game is

$$H = \lambda_z[B(t_f, t)u + C(t_f, t)v] \tag{19}$$

where λ_z is the costate variable satisfying

$$\dot{\lambda}_z = -\frac{\partial H}{\partial Z} = 0 \tag{20}$$

$$\lambda_z(t_f) = \left.\frac{\partial J}{\partial Z}\right|_{t_f} = \text{sign}\{Z(t_f)\}, \qquad Z(t_f) \neq 0 \tag{21}$$

which means that

$$\lambda_z(t) = \text{sign}\{Z(t_f)\}, \qquad Z(t_f) \neq 0 \tag{22}$$

as long as $\lambda_z(t)$ is continuous. This allows determining the optimal strategies as

$$u^* = \arg\min H = -\text{sign}\{B(t_f, t)Z(t_f)\}, \qquad Z(t_f) \neq 0 \tag{23}$$

$$v^* = \arg\max H = \text{sign}\{C(t_f, t)Z(t_f)\}, \qquad Z(t_f) \neq 0 \tag{24}$$

By assuming that $B(t_f, t) < 0$ and $C(t_f, t) > 0$, the optimal strategies become

$$u^* = v^* = \text{sign}\{Z(t_f)\}, \qquad Z(t_f) \neq 0 \tag{25}$$

Substituting Eq. (25) into Eq. (15) yields the optimized game dynamics

$$\dot{Z}^* = \Gamma(t_f, t)\text{sign}\{Z(t_f)\}, \qquad Z(t_f) \neq 0 \tag{26}$$

with

$$\Gamma(t_f, t) = [B(t_f, t) + C(t_f, t)] \tag{27}$$

Game Solution Structure

Integrating Eq. (26) backward from any given end condition $Z(t_f)$ generates a candidate optimal trajectory. The family of these trajectories determines the structure of the game solution. In this subsection, a review of some possible solution structures, presented first in a recent conference paper,[13] is outlined.

Case 1: $\Gamma(t_f, t) > 0 \;\; \forall\, t \in [t_0, t_f]$

Two families of monotonic optimal trajectories with opposite signs are generated, filling the entire game space (Fig. 4). The two trajectory families intersect on the $Z = 0$ axis, which serves as a dispersal line, dominated by the evader. In this case the optimal strategies (25) can be expressed in a state feedback form,

$$u^* = v^* = \text{sign}\{Z\} \qquad \forall\, Z \neq 0 \tag{28}$$

and the value of the game is a function of the initial conditions:

$$J^*(Z_0, t_0) = |Z_0| + \int_{t_0}^{t_f} \Gamma(t_f, t)\, \mathrm{d}t \tag{29}$$

Case 2: $\Gamma(t_f, t) = 0 \;\; \forall\, t \in [t_0, t_f]$

The entire game space is filled with optimal trajectories that are actually straight lines (Fig. 5). In this case the optimal strategies (25) in all of the game space, excluding the $Z = 0$ axis, can be expressed in a state feedback form,

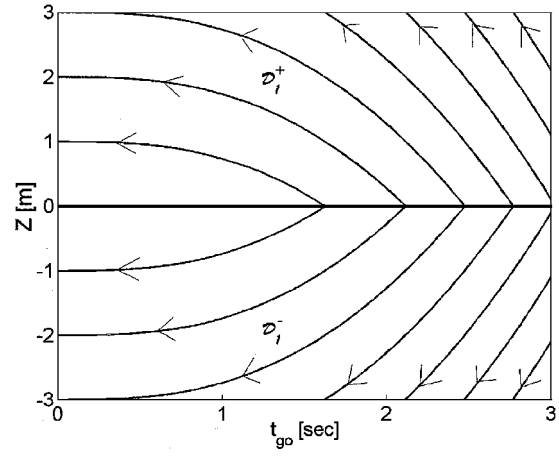

Fig. 4 Game space decomposition for case 1.

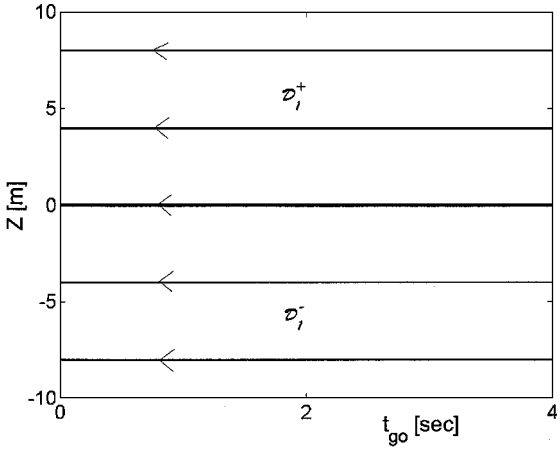

Fig. 5 Game space decomposition for case 2.

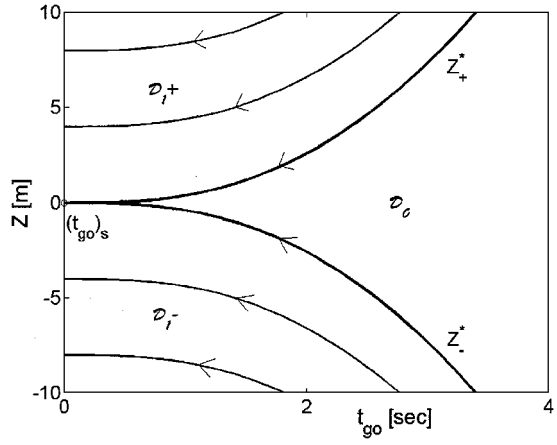

Fig. 6 Game space decomposition for case 3.

$$u^* = v^* = \text{sign}\{Z\} \qquad \forall\, Z \neq 0 \tag{30}$$

The $Z=0$ axis is a singular surface separating two regions with different gradients of the value function; the optimal evader's strategy is arbitrary, whereas the pursuer has to match this strategy. The value of the game is a function of the initial conditions:

$$J^*(Z_0, t_0) = |Z_0| \tag{31}$$

Case 3: $\Gamma(t_f, t) < 0\ \forall\ t \in [t_0, t_f)$

The optimal trajectory pair generated from the point $Z(t_f)=0$ with different signs separates the game space into two regions of different solutions (Fig. 6). Outside of these two optimal boundary trajectories, Z_+^* and Z_-^*, respectively, there is the region of regular trajectories $\mathcal{D}_1$, where the solution is given by Eqs. (28) and (29). The boundary trajectories themselves belong to $\mathcal{D}_1$. Inside the other region, denoted by $\mathcal{D}_o$ and defined by

$$|Z(t)| < Z_+^*(t) \tag{32}$$

the optimal strategies are arbitrary, and the value of the game is constant:

$$J_0^*(Z_0, t_0) = 0 \tag{33}$$

Inside this region, $\lambda_z(t)$, which represents the gradient of the value function, is identically zero. Thus, the game space is decomposed into three regions of different constant gradients (+1, −1, and 0) separated by the two semipermeable optimal boundary trajectories Z_+^* and Z_-^*, which are the singular surfaces of the game.

Case 4: $\Gamma(t_f, t) < 0,\ t \in [t_0, t_s);\ \Gamma(t_f, t) > 0,\ t \in (t_s, t_f)$

The optimal trajectories have an extremum at $t=t_s$. As a backward-generated candidate optimal trajectory intersects the $Z=0$ axis, it ceases to be optimal because the change in sign$\{Z\}$. The two families of such trajectories define a dispersal line of the game dominated by the evader. The boundary trajectories Z_+^* and Z_-^* are the pair of optimal trajectories that reach the $Z=0$ axis tangentially at $t=t_s$, which is the solution of $\Gamma(t_f, t)=0$. The two regions of the different game solutions shown in Fig. 7 are

$$\mathcal{D}_1 = \left\{(Z,t) : |Z(t)| \geq Z_+^*(t) \cup t_f \geq t \geq t_s\right\} \tag{34}$$

$$\mathcal{D}_o = \left\{(Z,t) : |Z(t)| < Z_+^*(t) \cap t < t_s\right\} \tag{35}$$

In $\mathcal{D}_1$, the optimal strategies and value of the game are given by Eqs. (28) and (29), respectively. In $\mathcal{D}_o$, the optimal strategies are arbitrary. Every trajectory that starts in this region must go through the throat $(Z,t)=(0,t_s)$. Consequently, the value of the game is constant:

$$J_0^*(Z_0, t_0) = \int_{t_s}^{t_f} \Gamma(t_f, t)\, \mathrm{d}t \triangleq M_s \tag{36}$$

The boundary trajectories and the dispersal line $\{Z(t)=0$ for $t_f \geq t \geq t_s\}$, dominated by the evader, belong to $\mathcal{D}_1$.

Case 5: $\Gamma(t_f, t) > 0,\ t \in [t_0, t_s);\ \Gamma(t_f, t) < 0,\ t \in (t_s, t_f)$

The two optimal trajectories generated from the point $Z(t_f)=0$ with different signs intersect again on the $Z=0$ axis at $t=t_c<t_s$ (assuming $t_c > t_0$) and enclose the $\mathcal{D}_o$ region (Fig. 8). All other optimal trajectory pairs, terminating at different values of $|Z(t_f)| \neq 0$, will also intersect each other on the $Z=0$ axis at $t<t_c$ (if t_f is large enough) creating an evader-dominated dispersal line $\{Z(t)=0\}$ for $t_0 \leq t \leq t_c$. Inside $\mathcal{D}_o$, the optimal strategies are arbitrary and the

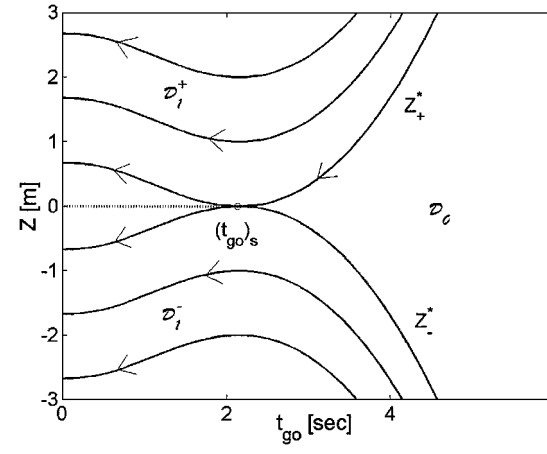

Fig. 7 Game space decomposition for case 4.

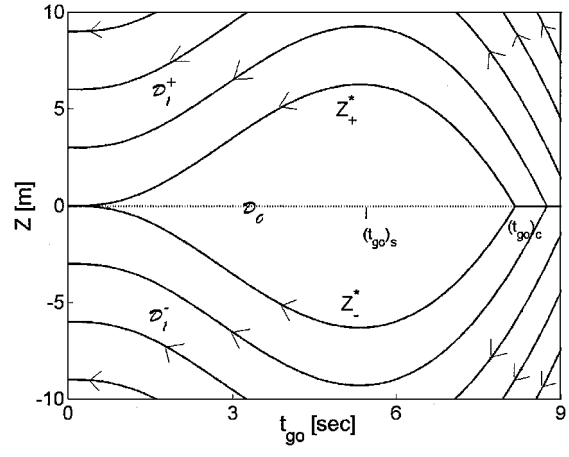

Fig. 8 Game space decomposition for case 5.

value of the game is zero. Elsewhere, that is, in $\mathcal{D}_1$, the game solution is given by Eqs. (28) and (29).

Remarks:

1) Particular examples where cases 1, 2, and 3 can occur are mentioned first in Ref. 9, using a simplified model, where both players have constant velocities and lateral acceleration limits, as well as ideal dynamics. Case 4 first appeared in Ref. 10, whereas case 5 was first presented in a recent conference paper.[13]

2) Other cases, where $\Gamma(t_f, t)$ changes its sign more than once, can also occur. These cases are out of the scope of the present paper.

3) In a game model with constant velocities and constant bounds on the lateral acceleration, solved in the Appendix, the conditions which lead to the different cases can be easily determined (see Table A1).

Explicit Computation of *Z*

To compute $\Gamma(t_f, t)$ for the present problem, the explicit expression for the zero effort miss distance is needed. For this purpose the homogeneous solution of Eq. (6) is derived step by step:

$$x_3(t) = x_3(t_0)\exp\{-[(t-t_0)/\tau_P]\} \tag{37}$$

$$x_4(t) = x_4(t_0)\exp\{-[(t-t_0)/\tau_E]\} \tag{38}$$

$$x_5(t) = x_5(t_0) + x_3(t_0) I_P(t, t_0) \tag{39}$$

$$x_6(t) = x_6(t_0) + x_4(t_0) I_E(t, t_0) \tag{40}$$

where

$$I_P(t, t_0) \triangleq \int_{t_0}^{t} \frac{\exp[-(\zeta/\tau_p)]}{V_p(\zeta)}\,\mathrm{d}\zeta \tag{41}$$

$$I_E(t, t_0) \triangleq \int_{t_0}^{t} \frac{\exp[-(\zeta/\tau_E)]}{V_E(\zeta)}\,\mathrm{d}\zeta \tag{42}$$

The integrals (41) and (42) have an analytic form only for very special cases of $V_P(t)$ and $V_E(t)$, respectively. Otherwise they have to be computed numerically. Substituting Eqs. (37–40) into the original equation (6) and integrating yields

$$\begin{aligned} x_2(t) &= x_2(t_0) + x_3(t_0)\tau_p\{\exp[-(t-t_0)/\tau_p] - 1 - II_P(t, t_0)\} \\ &\quad - x_4(t_0)\tau_E\{\exp[-(t-t_0)/\tau_E] - 1 - II_E(t, t_0)\} \\ &\quad - x_5(t_0)\cdot[V_P(t) - V_P(t_0)] + x_6(t_0)\cdot[V_E(t) - V_E(t_0)] \end{aligned} \tag{43}$$

where

$$II_P(t, t_0) \triangleq \int_{t_0}^{t} \frac{I_P(\zeta, t_0) a_{xP}(\zeta)}{\tau_P}\,\mathrm{d}\zeta \tag{44}$$

$$II_E(t, t_0) \triangleq \int_{t_0}^{t} \frac{I_E(\zeta, t_0) a_{xE}(\zeta)}{\tau_E}\,\mathrm{d}\zeta \tag{45}$$

Similarly, x_1 becomes

$$\begin{aligned} x_1(t) &= x_1(t_0) + x_2(t_0)(t-t_0) \\ &\quad - x_3(t_0)\tau_p^2\{\exp[-(t-t_0)/\tau_p] + (t-t_0)/\tau_p - 1 + III_P(t, t_0)\} \\ &\quad + x_4(t_0)\tau_E^2\{\exp[-(t-t_0)/\tau_E] + (t-t_0)/\tau_E - 1 + III_E(t, t_0)\} \\ &\quad - x_5(t_0)[IV_P(t, t_0) - V_P(t_0)(t-t_0)] \\ &\quad + x_6(t_0)[IV_E(t, t_0) - V_E(t_0)(t-t_0)] \end{aligned} \tag{46}$$

where

$$III_P(t, t_0) \triangleq \int_{t_0}^{t} \frac{II_P(\zeta, t_0)}{\tau_P}\,\mathrm{d}\zeta, \qquad IV_P(t, t_0) \triangleq \int_{t_0}^{t} V_P(\zeta)\,\mathrm{d}\zeta \tag{47}$$

$$III_E(t, t_0) \triangleq \int_{t_0}^{t} \frac{II_E(\zeta, t_0)}{\tau_E}\,\mathrm{d}\zeta, \qquad IV_E(t, t_0) \triangleq \int_{t_0}^{t} V_E(\zeta)\,\mathrm{d}\zeta \tag{48}$$

Thus, the zero effort miss distance of the general time variable problem is

$$\begin{aligned} Z(t) &= x_1(t) + x_2(t)t_{\mathrm{go}} - x_3(t)\tau_P^2\{\exp[-(t_{\mathrm{go}}/\tau_p)] + (t_{\mathrm{go}}/\tau_p) \\ &\quad - 1 + III_P(t_f, t)\} + x_4(t)\tau_E^2\cdot\{\exp[-(t_{\mathrm{go}}/\tau_E)] + (t_{\mathrm{go}}/\tau_E) \\ &\quad - 1 + III_E(t_f, t)\} - x_5(t)[IV_P(t_f, t) - V_P(t)t_{\mathrm{go}}] \\ &\quad + x_6(t)[IV_E(t_f, t) - V_E(t)t_{\mathrm{go}}] \end{aligned} \tag{49}$$

Comparing this expression to the one obtained for the time-invariant model, as given in the Appendix, Eq. (A3), one can observe that there are separate correction terms for the pursuer and the evader. The integrals $III_P(t_f, t)$ and $III_E(t_f, t)$ express the effects of the respective longitudinal accelerations, whereas the terms with the additional state variables $x_5(t)$ and $x_6(t)$ represent the resulting changes in the respective velocity components normal to the LOS.

After eliminating equal terms, the time derivative of Eq. (49) becomes

$$\begin{aligned} \frac{\mathrm{d}Z}{\mathrm{d}t} &= v\cdot a_E^{\max}(t)\left\{\exp\left[-\left(\frac{t_{\mathrm{go}}}{\tau_E}\right)\right] + \left(\frac{t_{\mathrm{go}}}{\tau_E}\right) - 1 + III_E(t_f, t)\right\}\tau_E \\ &\quad - u\cdot a_P^{\max}(t)\left\{\exp\left[-\left(\frac{t_{\mathrm{go}}}{\tau_P}\right)\right] + \left(\frac{t_{\mathrm{go}}}{\tau_P}\right) - 1 + III_P(t_f, t)\right\}\tau_P \end{aligned} \tag{50}$$

Substituting Eq. (25) into Eq. (50) yields the optimal game dynamics

$$\frac{\mathrm{d}Z^*}{\mathrm{d}t} = \Gamma(t_f, t)\cdot\mathrm{sign}(Z) \qquad \forall\, Z \neq 0 \tag{51}$$

where

$$\begin{aligned} \Gamma(t_f, t) &= a_E^{\max}(t)\{\exp[-(t_{\mathrm{go}}/\tau_E)] + (t_{\mathrm{go}}/\tau_E) - 1 + III_E(t_f, t)\}\tau_E \\ &\quad - a_P^{\max}(t)\{\exp[-(t_{\mathrm{go}}/\tau_P)] + (t_{\mathrm{go}}/\tau_P) - 1 + III_P(t_f, t)\}\tau_P \end{aligned} \tag{52}$$

Note that in the derivation of the general solution it was assumed that $B(t_f, t) < 0$ and $C(t_f, t) > 0$. These assumptions are valid in the investigated end-game scenario. For $a_{xP}(t) > 0$, obviously $II_P(t_f, t)$ of Eq. (44) is positive and consequently, $III_P(t_f, t)$ of Eq. (47) is also positive. The same is true for $a_{xE} > 0$, and it follows immediately that $B(t_f, t)$ of Eq. (16) is negative and $C(t_f, t)$ of Eq. (17) is positive. For $a_{xP}(t) < 0$ and/or $a_{xE}(t) < 0$ the validity of the inequalities $B(t_f, t) < 0$ and $C(t_f, t) > 0$ have to be tested.

Simplified Example

In typical TBM interception scenarios, which have served as the motivation of the present study, the velocity and maneuverability profiles have similar time-varying features to those presented in Figs. 1 and 2. For such scenarios two simplifying assumptions can be made.

1) The engagement is between an interceptor missile with a constant longitudinal acceleration [$a_{xP}(t) = a_{xP}$] and a constant speed reentering TBM [$a_{xE}(t) = 0$].

2) The lateral acceleration limit of the interceptor is constant, whereas that of the evader is linearly time varying.

Based on simplifying assumption 1, the pursuer's velocity can be expressed as

$$V_p(t) = V_{\mathrm{pf}}(1 - \alpha t_{\mathrm{go}}/\tau_P) \tag{53}$$

where V_{pf} is the pursuer's final velocity and

$$\alpha = a_{xp}\tau_p/V_{\mathrm{pf}} \tag{54}$$

Based on simplifying assumption 2, the evader's maneuverability can be expressed as

$$a_E^{\max}(t) = a_{Ef}^{\max}[1 - \beta t_{\mathrm{go}}/\tau_P] \tag{55}$$

The zero effort miss distance in this simplified example is

$$Z^{\alpha\beta} = Z^1 + \Delta Z^{\alpha\beta} \tag{56}$$

where Z^1 is the zero effort miss distance for the constant speed model [Eqs. (A3–A5)] and

$$\Delta Z^{\alpha\beta} = -\left[III_P(t_{\rm go})\tau_p^2 x_3 + 0.5\alpha t_{\rm go}^2 V_{\rm pf} x_5 \big/ \tau_p\right] \tag{57}$$

with

$$III_P(t_{\rm go}) = \int_0^{t_{\rm go}} {\rm d}\xi \int_0^{\xi} {\rm d}\varsigma \int_0^{\varsigma} \frac{\alpha \exp[-(\zeta/\tau_P)]}{\tau_P^2[1-\alpha(\zeta/\tau_P)]}\,{\rm d}\zeta \tag{58}$$

Note that in this simplified example the only state variables that effect the change of the zero effort miss distance are $x_3(a_p)$ and $x_5(\phi_p)$, both belonging to the pursuer. With the use of the new definition of the zero effort miss distance (56), the optimal strategies become

$$u^* = v^* = \text{sign}\{Z^{\alpha\beta}\} \tag{59}$$

The time-varying evader maneuverability does not effect these optimal strategies, but modifies the dynamics and the outcome of the engagement. The resulting dynamics along the optimal trajectories are

$$\frac{{\rm d}Z^{\alpha\beta^*}}{{\rm d}t} = \Gamma^{\alpha\beta}(t_f, t)\cdot \text{sign}(Z^{\alpha\beta}) \tag{60}$$

where

$$\Gamma^{\alpha\beta}(t_f, t) = a_{Ef}^{\max}\{\exp[-(t_{\rm go}/\tau_E)] + (t_{\rm go}/\tau_E) - 1\}\tau_E[1-\beta t_{\rm go}/\tau_P] - a_P^{\max}\{\exp[-(t_{\rm go}/\tau_P)] + (t_{\rm go}/\tau_P) - 1 + III_P(t_{\rm go}/\tau_P)\}\tau_P \tag{61}$$

The nonvanishing solution of the equation $\Gamma^{\alpha\beta} = 0$ (if it exists) provides $(t_{\rm go})_s^{\alpha\beta} > 0$, and the value of the game in region $\mathcal{D}_0$ is

$$M_s^{\alpha\beta} = \int_0^{(t_{\rm go})_s} \Gamma^{\alpha\beta}\,{\rm d}t \tag{62}$$

The effect of the normalized parameters α and β defined by Eqs. (54) and (55), on the critical time to go $(t_{\rm go})_s^{\alpha\beta}$ and on the guaranteed miss distance $M_s^{\alpha\beta}$ is shown in Figs. 9 and 10, respectively. It can be seen from Fig. 10 that the guaranteed miss distance decreases as α increases. The reason is that the velocity vector is generally not aligned with the LOS, and consequently, a positive longitudinal acceleration ($\alpha > 0$) has a component normal to it, which augments the pursuer maneuverability and results in smaller miss distances. An increase in β also results in a decrease of the guaranteed miss distance because the effective maneuverability ratio during the end game is smaller than its final value used in Eq. (55).

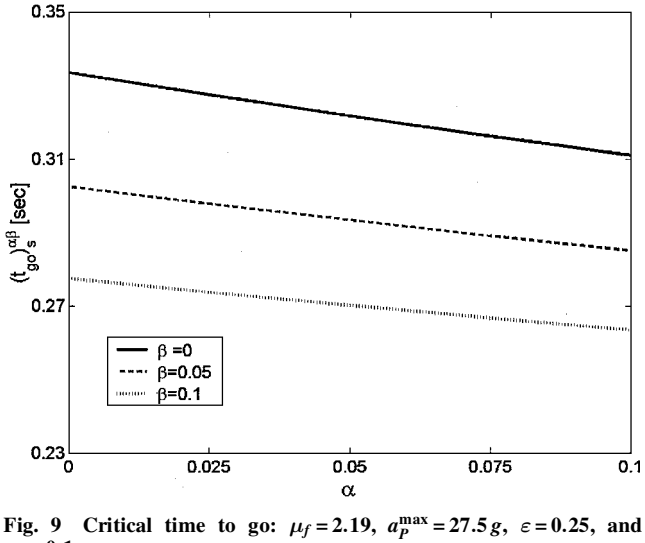

Fig. 9 Critical time to go: $\mu_f = 2.19$, $a_P^{\max} = 27.5\,g$, $\varepsilon = 0.25$, and $\tau_E = 0.1$ s.

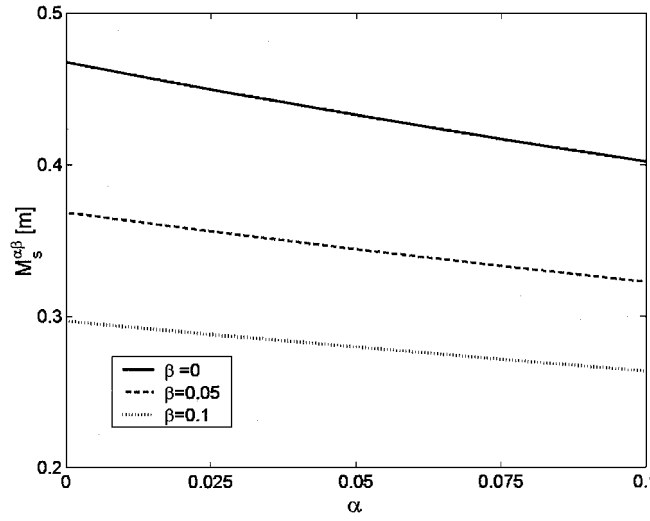

Fig. 10 Guaranteed miss distance: $\mu_f = 2.19$, $a_P^{\max} = 27.5\,g$, $\varepsilon = 0.25$, and $\tau_E = 0.1$ s.

Validation Study

Scenario Description

In the simulated scenario, a single interceptor missile is launched against a reentering TBM of high maneuverability. This scenario was analyzed in great detail in Ref. 1 and compared to the originally used simplified (constant velocity) linear model, which motivated the present study. The results presented in this paper were obtained by the same simulation program, and its main features are repeated here for the sake of completeness.

The simulation program consists of the following elements: three-dimensional nonlinear relative kinematics between two point-mass vehicles, point-mass dynamics of both missiles, simplified guidance and control dynamics of each vehicle, and a high-altitude standard atmospheric model. The simulations are carried out in a fixed Cartesian coordinate system, assuming flat nonrotating Earth and no wind. The well-known equations of three-dimensional kinematics and point-mass dynamics of atmospheric flying vehicles are summarized in Ref. 14 and are not repeated here.

For the sake of simplicity, a point defense scenario is considered, that is, the interceptor missile is launched from the vicinity of the TBM's target. The initial position of the TBM is determined by assuming a nonmaneuvering ballistic trajectory aimed at a fixed surface target. The initial position of the TBM also determines the vertical plane of reference. When the reentering TBM is detected, the defense system selects the desired altitude for interception and launches a guided missile toward the predicted point of impact at this altitude. In this study a nominal interception altitude of 22 km is selected. The velocity and maximum lateral acceleration profiles along the nominal (nonmaneuvering) trajectory are plotted in Figs. 1 and 2, respectively.

The results presented in this paper concentrate on the interception end game, where a sequence of hard TBM maneuvers is assumed to take place. This end game starts when the TBM crosses the altitude of 28 km and has an approximate duration of 3 s. The initial TBM maneuver is commanded in the horizontal plane (either right or left). The sequence is completed by a second maneuver, commanded to the opposite direction, after some time $\Delta t_{sw} \in [0, 3]$ s. The values of Δt_{sw} vary between different simulation runs in steps of approximately 0.25 s corresponding to steps of 500 m of altitude.

These types of end-game maneuver sequences were selected because both optimal control[15] and differential game[9–11] theories predict that the optimal missile avoidance maneuver (aimed to maximize the miss distance) has such a bang–bang structure. Moreover, these maneuvers with varying Δt_{sw}, represent adequately the ensemble of the random maneuver samples that can be implemented by the designer of a TBM without the knowledge of the interception altitude. In the next subsections the specific guidance and control models of a maneuvering TBM and the interceptor missile are described.

TBM Model

The reentering TBM is assumed to be a generic cruciform flying vehicle having some control surfaces to execute lateral maneuvers up to a given angle of attack $\alpha_{\max}$ in nonrolling body coordinates. The relationship between the actual angle of attack and its commanded value is approximated by a first-order transfer function with a time constant $\tau_E \in [0.01, 0.4]$ s. The generic TBM used in this study is characterized by its ballistic coefficient ($b = 5000$ kg/m^2), which determines the deceleration in the atmosphere and the lift to drag ratio $\Lambda \in [1.41, 2.83]$ at the angle of attack generating maximum lift.

Interceptor Model

The generic interceptor missile (designed for high endoatmospheric interception) has an aerodynamically controlled cruciform airframe and is assumed to be roll stabilized. It has a two-stage solid rocket propulsion. Each rocket motor provides a constant thrust. After the burnout of the first stage, the booster is separated, and the second rocket motor is ignited. The maneuverability of the missile (its lateral acceleration and the corresponding load factor) is limited, in each of the two perpendicular planes of the cruciform configuration, by the maximum lift coefficient. It is assumed that the missile's autopilot can be represented by a first-order transfer function with a time constant $\tau_P \in [0.05, 0.4]$ s. The parameters of the interceptor are summarized in Table 1, where SC_D and $SC_{L\max}$ are the drag and maximum lift coefficients multiplied by the surface of reference respectively.

The guidance system of the interceptor missile consists of two identical, decoupled channels, associated with the perpendicular planes of the cruciform configuration. Because the missile is roll stabilized, one channel is designated to perform lateral accelerations in the vertical plane and the other in the direction perpendicular to it. An appropriate missile's guidance law generates the acceleration command for each channel subject to the saturation imposed by the maximum lift coefficient.

In the present study two different differential games guidance laws are considered: 1) DGL/1, which is based on the linear model of constant speeds and lateral acceleration limits,[11] and 2) DGL/E, which is derived using the extended time-varying linear model and the simplifying assumptions 1 and 2, (both well justified in this example) presented in this paper.

The new guidance law based on the extended linear model leads to a substantial improvement of the homing accuracy in a representative TBM interception scenario with time-varying missiles velocities and lateral acceleration limits, as demonstrated by the results of the three-dimensional nonlinear simulation shown in Figs. 11 and 12. In Fig. 11 the robust behavior of DGL/E is clearly seen. Moreover, the extended linear model provides a much more accurate prediction of the miss distance obtained by the three-dimensional nonlinear simulation, as shown in Fig. 13. The negligible differences confirm the validity of the simplified DGL/E model in this example.

Table 1 Interceptor data

Stage	Burning time, s	Thrust, kN	Initial mass, kg	Final mass, kg	SC_D, m^2	$SC_{L\max}$, m^2
1	6.5	229.0	1540.0	933.0	0.10	0.24
2	13.0	103.0	781.0	236.0	0.05	0.20

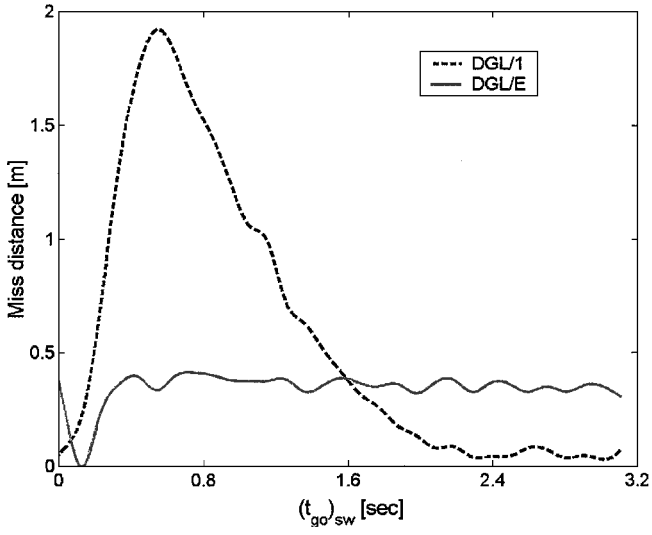

Fig. 11 Miss distance vs $(t_{go})_{sw}$: $\mu_f = 2.19$, $a_P^{\max} = 27.5\,g$, $\varepsilon = 0.25$, $\tau_E = 0.1$ s, $\alpha = 0.034$, and $\beta = 0.074$.

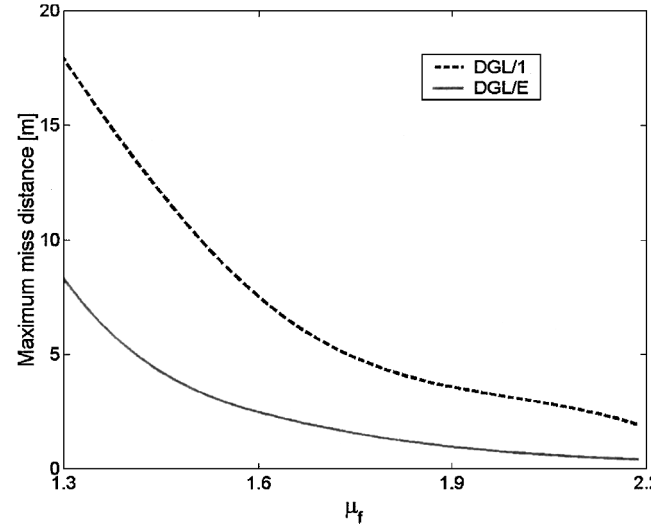

Fig. 12 Maximum miss distance vs final maneuverability ratio: $a_P^{\max} = 27.5\,g$, $\varepsilon = 0.25$, $\tau_E = 0.1$ s, $\alpha = 0.034$, and $\beta = 0.074$.

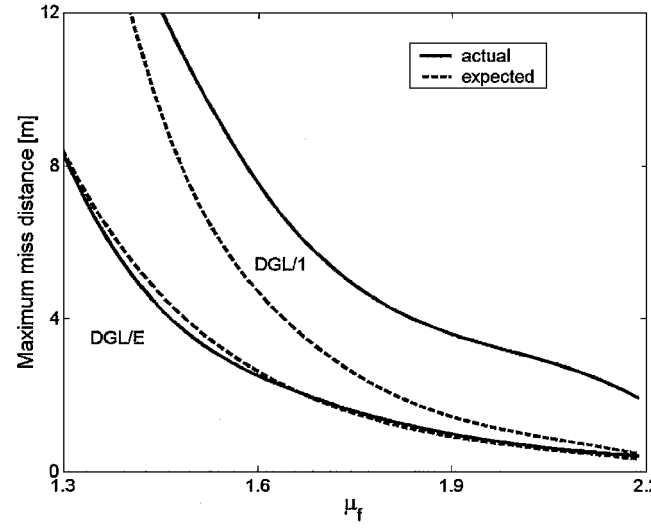

Fig. 13 Predicted vs actual mass distances for DGL/1 and DGL/E: $a_P^{\max} = 27.5\,g$, $\varepsilon = 0.25$, $\tau_E = 0.1$ s, $\alpha = 0.034$, and $\beta = 0.074$.

Conclusions

A time-varying linear pursuit–evasion game model with bounded controls has been presented. The linear game model allows applying the method of terminal projection, which reduces the dimension of the game dynamics and leads to a single state variable (the zero-effort miss distance). This model has been used for the development of a new interceptor guidance law based on differential game theory.

The derived guidance law has been tested in a three-dimensional nonlinear point-mass simulation of a realistic BMD scenario, where the velocities and lateral acceleration limits of both missiles are time varying. It has been shown that using this guidance law provides significant improvements in the homing accuracy (at least 50% in the simulated scenarios) compared to a differential game guidance law derived assuming constant velocities and lateral acceleration limits. Moreover, the extended linear model provides a much more

accurate prediction of the miss distance, confirming its validity even if simplifying assumptions are introduced.

It is important to emphasize that although the time-varying linear pursuit–evasion game model was motivated for analyzing a BMD scenario, it can be also used in other interception problems of interest. The assumption of known velocity and maneuverability profiles seem to have some limitations. However, the parts of the guidance law corrections that depend on the interceptor are either known or can be directly measured with relatively small errors. The lateral and longitudinal velocity and acceleration components of the target have to be estimated in any case based on noisy measurements. The velocity and maneuverability profiles of the target are very much scenario dependent (they may not be as easily predictable as in a BMD scenario), but any judicious assumption for these profiles will certainly improve the accuracy of the guidance and the miss distance prediction compared to using a model with constant parameters.

The game solution leading to the guidance law derivation is based on the decomposition of the reduced game space. In this paper, a general review of possible structures of the game space decomposition is presented. One of these structures implies that even if the pursuer does not have a maneuverability advantage over the evader, but has an agility advantage (agility is defined as the maximum lateral acceleration divided by the time constant of the missile), a zero miss distance still can be achieved for some initial conditions.

Appendix: Game with Constant Maneuverability and Velocity

This game has served as a simplified linearized model for the terminal phase of intercepting a maneuvering target by a guided missile.[11] The game solution is based on the assumptions that both players have constant velocities and the bounds on their lateral accelerations are also constant. Consequently, the pursuer–evader maneuverability ratio, defined as

$$\mu = a_P^{\max} \big/ a_E^{\max} \tag{A1}$$

is constant and serve together with the evader–pursuer dynamics ratio, defined as

$$\varepsilon = \tau_E / \tau_P \tag{A2}$$

as the parameters of the game. The product of these two parameters is called the pursuer–evader agility ratio, where the term agility is defined as the maximum lateral acceleration divided by the time constant of the missile. It is also assumed that the interception takes place in a plane with small deviations from the initial LOS (ILOS). The equations of motion are written in Cartesian coordinates, where the X axis is aligned with ILOS. The assumptions of constant speed and trajectory linearization allow solving the equation of motion in the X direction as a function of time to go. Therefore, only the equations of motion in the Y direction (perpendicular to the ILOS) remain to be solved.

If both players have first-order dynamics,[11] the game (called in the recent literature DGL/1 and its variables will be denoted with the superscript 1) has the first four state variables of Eq. (3). The terminal projection transformation leads to the definition of the zero effort miss distance as

$$Z^1(t) = x_1(t) + x_2(t)t_{\text{go}} + \Delta Z_E(t) - \Delta Z_P(t) \tag{A3}$$

where

$$\Delta Z_E(t) = \tau_E^2[\exp(-t_{\text{go}}/\tau_E) + t_{\text{go}}/\tau_E - 1]x_4(t) \tag{A4}$$

$$\Delta Z_p(t) = \tau_p^2[\exp(-t_{\text{go}}/\tau_P) + t_{\text{go}}/\tau_P - 1]x_3(t) \tag{A5}$$

The optimized game dynamics is

$$\frac{\mathrm{d}Z^{1*}}{\mathrm{d}t} = \Gamma^1 \cdot \operatorname{sign}[Z^1(t)] \tag{A6}$$

Table A1 Conditions for various game solution structures

Agility ratio	$\mu < 1$	$\mu = 1$	$\mu > 1$
$\mu\varepsilon < 1$	Case 1 (Fig. 4)	Case 1 (Fig. 4)	Case 4 (Fig. 7)
$\mu\varepsilon = 1$	Case 1 (Fig. 4)	Case 2 (Fig. 5)	Case 3 (Fig. 6)
$\mu\varepsilon > 1$	Case 5 (Fig. 8)	Case 3 (Fig. 6)	Case 3 (Fig. 6)

where

$$\Gamma^1 = -a_P^{\max}[\exp(-t_{\text{go}}/\tau_P) + t_{\text{go}}/\tau_P - 1]\tau_P + a_E^{\max}[\exp(-t_{\text{go}}/\tau_E) + t_{\text{go}}/\tau_E - 1]\tau_E \tag{A7}$$

The game space can have five different structures depending on the maneuverability ratio μ and the agility ratio $\mu\varepsilon$, as shown in Table A1.

In all of these cases, the guaranteed miss distance in region $\mathcal{D}_1$ depends on the initial conditions, as well as on the parameters μ and ε. The region $\mathcal{D}_0$ exists only in cases 3–5. The guaranteed miss distance for this entire region depends only on the parameters μ and ε:

$$M_s^1 = a_E^{\max}\tau_P^2\left\{\mu(1-\varepsilon)\left(\exp\left[-(t_{\text{go}})_s^1\big/\tau_P\right] + (t_{\text{go}})_s^1\big/\tau_P - 1\right) - (\mu-1)\left[(t_{\text{go}})_s^1\big/\tau_P\right]^2\Big/2\right\} \tag{A8}$$

where $(t_{\text{go}})_s^1$ is the strictly positive solution of the equation $\Gamma^1 = 0$. In case 3, both $(t_{\text{go}})_s^1$ and M_s^1 are identically zero.

Note that case 5 implies that even if the pursuer does not have a maneuverability advantage ($\mu < 1$) over the evader, the pursuer may still achieve a hit-to-kill for some initial conditions, if it has an agility advantage ($\mu\varepsilon > 1$).

Acknowledgment

This work was supported in part by the U.S. Air Force under Contract AFOSR-F61708-97-C0004.

References

[1] Shinar, J., Shima, T., and Kebke, A., "On the Validity of Linearized Analysis in the Interception of Reentry Vehicles," *Proceedings of the AIAA Guidance, Navigation, and Control Conference*, AIAA, Reston, VA, 1998, pp. 1050–1060.

[2] Garnell, P., *Guided Weapon Control Systems*, Pergamon, New York, 1980, pp. 238–240.

[3] Zarchan, P., *Tactical and Strategic Missile Guidance*, Vol. 176, Progress in Astronautics and Aeronautics, AIAA, Reston, VA, 1997, pp. 11–29.

[4] Baba, Y., Takehira, T., and Takano, H., "New Guidance Law for a Missile with Varying Velocity," *Proceedings of the AIAA Guidance, Navigation, and Control Conference*, AIAA, Washington, DC, 1994, pp. 207–215.

[5] Riggs, T., "Linear Optimal Guidance for Short Range Air to Air Missile," *Proceedings of the National Aerospace Electronics Conference*, Vol. 2, 1979, pp. 757–764.

[6] Lee, G. F. K., "Estimation of the Time-to-Go Parameter for Air-to-Air," *Journal of Guidance, Control, and Dynamics*, Vol. 8, No. 2, 1985, pp. 262–266.

[7] Cho, H., Ryoo, C. K., and Tahk, M. J., "Closed-Form Optimal Guidance Law for Missiles of Time-Varying Velocity," *Journal of Guidance, Control, and Dynamics*, Vol. 19, No. 5, 1996, pp. 1017–1022.

[8] Garber, V., "Optimum Intercept Laws for Accelerating Targets," *AIAA Journal*, Vol. 6, No. 11, 1968, pp. 2196–2198.

[9] Gutman, S., and Leitmann, G., "Optimal Strategies in the Neighbourhood of a Collision Course," *AIAA Journal*, Vol. 14, No. 9, 1976, pp. 1210–1212.

[10] Gutman, S., "On Optimal Guidance for Homing Missiles," *Journal of Guidance and Control*, Vol. 3, No. 4, 1979, pp. 296–300.

[11] Shinar, J., "Solution Techniques for Realistic Pursuit-Evasion Games," *Advances in Control and Dynamic Systems*, Vol. 17, Academic Press, New York, 1981, pp. 63–124.

[12] Gazit, R., and Gutman, S., "Development of Guidance Laws for a Variable-Speed Missile," *Dynamics and Control*, Vol. 1, No. 2, 1991, pp. 177–198.

[13] Shima, T., and Shinar, J., "On the Extension of Linear Pursuit—Evasion Game Models Applied for Interception Analysis," *Proceedings of the 39th Israel Annual Conference on Aerospace Sciences*, 1999, pp. 142–152.

[14] Shinar, J., and Zarkh, M., "Interception of Maneuvering Tactical Ballistic Missiles in the Atmosphere," *Proceedings of the 19th ICAS Congress and AIAA Aircraft Systems Conference*, 1994, pp. 1354–1363.

[15] Shinar, J., and Steinberg, D., "Analysis of Optimal Evasive Maneuvers Based on a Linearized Two-Dimensional Kinematic Model," *Journal of Aircraft*, Vol. 14, No. 8, 1977, pp. 795–802.